Phototransformation of pesticides in the environment

11. PHOTOTRANSFORMATION OF PESTICIDES IN THE ENVIRONMENT

Davide Vione(*), Marco Minella, Claudio Minero

University of Torino, Department of Chemistry, Via Pietro Giuria 5, 10125 Torino, Italy.
Tel. +39-011-6705296; Fax +39-011-6705242; E-mail: davide.vione@unito.it

This chapter presents the main photoinduced transformation processes involving pesticides molecules in sunlit surface waters, on soil and in the atmosphere (taking into account both the gas and the condensed phase). Moreover, a recently developed model approach to predict pollutant phototransformation in surface waters is presented and described, together with an example referred to the herbicide MCPA (4-chloro-2-methylphenoxyacetic acid) and to the production of the toxic transformation intermediate 4-chloro-2-methylphenol.

11.1. PHOTOTRANSFORMATION OF PESTICIDES IN SURFACE WATERS

11.1.1. PHOTOCHEMICAL PROCESSES IN SURFACE WATERS

The photochemical processes that involve organic contaminants (including pesticides) in surface waters can be divided into direct photolysis and indirect or sensitized photochemistry. The direct photolysis in environmental waters takes place when a compound absorbs sunlight and when sunlight absorption causes transformation. Therefore, only sunlight-absorbing compounds can undergo direct photolysis in the environment [1].

Figure 11.1 gives some insight into the processes that follow radiation absorption by a molecule [2]. Assume that the substrate is initially in the ground vibrational level of the ground electronic state, S_o. For most organic molecules, S_o is a singlet state. Absorption of a photon can promote the molecule from S_o to a vibrationally excited state of an electronically excited singlet state. For simplicity, suppose that the electronically excited state is the first singlet state, S_1. After radiation absorption, the molecule reaches a vibrationally excited state of S_1. In some cases, the excess vibrational energy can be high enough to cause bond breaking that triggers the transformation of the molecule. Otherwise, vibrational energy can be lost by relaxation (*e.g.* by collisions with the solvent) to reach the ground vibrational state of S_1. If the vibrational relaxation is complete, *i.e.* if the molecule gets back to the ground vibrational state of S_o, one speaks of internal conversion. As an alternative, the molecule in the singlet state S_1 can undergo reactions that are, however, little likely due to the short lifetimes of the excited singlet states (usually in the sub-nanosecond level). Other possible pathways are emission of fluorescence radiation (at higher wavelength, that is, lower energy than the absorbed one) or the inter-system crossing (ISC) to a triplet state (in Figure 11.1 this is the first triplet state, T_1). The ISC is enabled by the fact that the T_1 energy is lower than that of S_1, but a vibrationally excited T_1 state can have the same or very similar energy as ground-state S_1. The following step is relaxation to the ground vibrational state of T_1, which can continue down to S_o (internal conversion). As an alternative, the state T_1 can undergo chemical reactions such as rearrangements, reactions with other dissolved molecules such as O_2, or reactions with the solvent. There is higher probability that T_1 reacts compared to S_1, because the triplet states are longer-lived than singlet ones (lifetimes are usually in the nanosecond-microsecond level). Some dissolved molecules (for instance humic and fulvic acids) have triplet states with oxidizing capability and can induce the degradation of other compounds, including organic

pollutants. They are called photosensitisers and their reactions will be dealt with more extensively when describing the indirect photolysis processes. A final option, which is mainly observed in solid systems or in deep-frozen solutions, is the emission of phosphorescence radiation.

In some cases, the energy of the absorbed radiation is so high that an electron is ejected out of the molecule. The corresponding phenomenon is called photoionisation and it is more common with low-wavelength radiation (*e.g.* UVC), but some molecules undergo photoionisation even with UVB or UVA radiation. The ionisation process is usually a first step that is followed by further reactions of the radical cation thus formed, *e.g.* reaction with the solvent.

Therefore, a sunlight-absorbing molecule can undergo direct photolysis by bond breaking (excess of vibrational energy), reactions involving S_1 or most notably T_1, and photoionisation. Such reactions can involve the molecule alone (intra-molecular processes) or other compounds including the solvent (inter-molecular processes) [2].

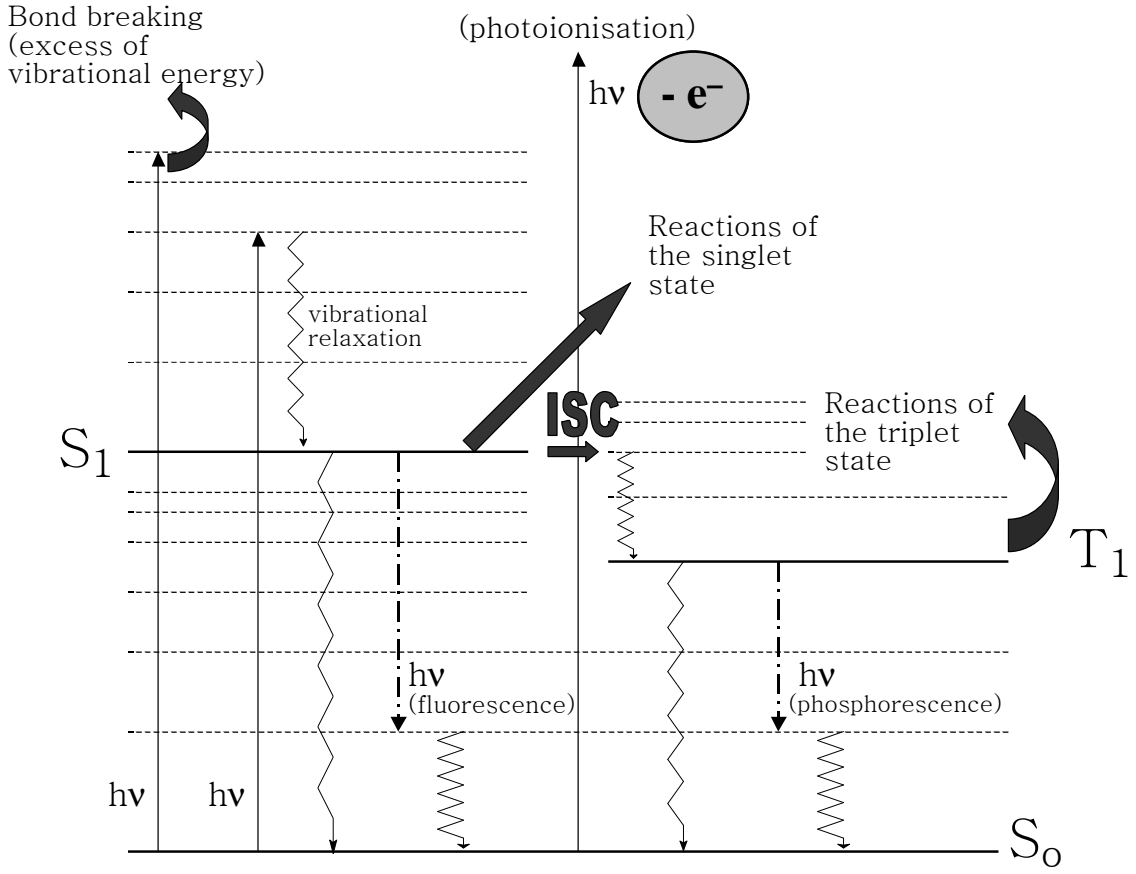

Figure 11.1 Schematic of the processes that may follow radiation absorption by a water-dissolved organic compound. Solid horizontal lines represent ground vibrational states of electronic levels, excited vibrational states being dashed. Solid and straight vertical arrows represent radiation absorption processes (hν = photon), zigzag arrows are vibrational relaxation processes, while dash-dotted arrows represent light emission (fluorescence or phosphorescence). ISC = inter-system crossing.

In the case of indirect or sensitised photolysis, sunlight is absorbed by photoactive compounds called photosensitisers. The latter produce photoactive transients upon radiation absorption, which can induce the degradation of dissolved compounds including organic pollutants. The main photosensitisers in surface waters are chromophoric dissolved organic matter (CDOM), nitrate, nitrite and, probably to a somewhat lesser extent, Fe species and hydrogen peroxide. Reactive transients that are photogenerated and can be involved in substrate degradation are the hydroxyl ($^{\bullet}OH$) and carbonate radicals ($CO_3^{-\bullet}$), singlet oxygen ($^1O_2$) and the triplet states of CDOM (^{3}CDOM*) [3,4]. The formation and reactivity of the various transients will now be discussed.

The $^{\bullet}OH$ radical is definitely the most reactive transient that occurs in surface waters. It is produced by photolysis of nitrate and nitrite [5] and by irradiation of CDOM. In the latter case there is still debate in the literature as to the possible pathway of $^{\bullet}OH$ generation: it could be oxidation of water or of OH^- by ^{3}CDOM* (reactions 4,5) [6], or a photo-Fenton process involving complexes between Fe(III) and organic ligands within CDOM (reactions 6-9) [7].

$$NO_3^- + h\nu + H^+ \rightarrow {}^{\bullet}NO_2 + {}^{\bullet}OH \quad (1)$$
$$NO_2^- + h\nu + H^+ \rightarrow {}^{\bullet}NO + {}^{\bullet}OH \quad (2)$$
$$CDOM + h\nu \rightarrow CDOM^* \text{—(ISC)}\rightarrow {}^3CDOM^* \quad (3)$$
$$^3CDOM^* + H_2O \rightarrow CDOM\text{-}H^{\bullet} + {}^{\bullet}OH \quad (4)$$
$$^3CDOM^* + OH^- \rightarrow CDOM^{-\bullet} + {}^{\bullet}OH \quad (5)$$
$$Fe^{III}\text{-}L + h\nu \rightarrow Fe^{2+} + L^{+\bullet} \quad (6)$$
$$Fe^{2+} + O_2 \rightarrow Fe^{3+} + O_2^{-\bullet} \quad (7)$$
$$2\ O_2^{-\bullet} + 2\ H^+ \rightarrow H_2O_2 \quad (8)$$
$$Fe^{2+} + H_2O_2 \rightarrow Fe^{3+} + {}^{\bullet}OH + OH^- \quad (9)$$

The radical $^{\bullet}OH$ undergoes very fast reactions with many water-dissolved compounds, including xenobiotics and natural organic molecules (natural dissolved organic matter, hereafter DOM) [8]. For this reason, the steady-state [$^{\bullet}OH$] in surface waters is very low (at or below 10^{-16} M) and this limits the importance of $^{\bullet}OH$ reactions in pollutant transformation. The main $^{\bullet}OH$ scavengers in surface waters are DOM, HCO_3^- and CO_3^{2-}, with nitrite also playing some (limited) role [9,10].

$$^{\bullet}OH + DOM \rightarrow Products \quad (10)$$
$$^{\bullet}OH + HCO_3^- \rightarrow H_2O + CO_3^{-\bullet} \quad (11)$$
$$^{\bullet}OH + CO_3^{2-} \rightarrow OH^- + CO_3^{-\bullet} \quad (12)$$
$$^{\bullet}OH + NO_2^- \rightarrow OH^- + {}^{\bullet}NO_2 \quad (13)$$

Reactions (11, 12) of $^{\bullet}OH$ with bicarbonate and carbonate yield the radical $CO_3^{-\bullet}$, which is also a reactive transient but a less powerful oxidant than $^{\bullet}OH$. The radical $CO_3^{-\bullet}$ can also be produced upon oxidation of carbonate by ^{3}CDOM* [4]:

$$^3CDOM^* + CO_3^{2-} \rightarrow CDOM^{-\bullet} + CO_3^{-\bullet} \quad (14)$$

Scavenging of $CO_3^{-\bullet}$ mainly takes place upon reaction with DOM. Note that reactions (11,12) are usually the main sources of $CO_3^{-\bullet}$ in surface waters, reaction (14) usually playing a secondary role. This means that the formation rate of $CO_3^{-\bullet}$ is lower compared to $^{\bullet}OH$, because the rate of $^{\bullet}OH$ formation equals that of its scavenging (steady-state condition) and the main $^{\bullet}OH$ scavenging process is reaction (10) with DOM. Indeed, reactions (11,12) yielding $CO_3^{-\bullet}$ from $^{\bullet}OH$ are secondary processes

of $^{\bullet}OH$ consumption in most natural waters. However, because the reaction rate constant between DOM and $CO_3^{-\bullet}$ is two-three orders of magnitude lower than the rate constant of $^{\bullet}OH$ with DOM, the steady-state [$CO_3^{-\bullet}$] in surface waters is often considerably higher than the steady-state [$^{\bullet}OH$]. The higher [$CO_3^{-\bullet}$] compared to [$^{\bullet}OH$] is usually compensated for by the lower reactivity of $CO_3^{-\bullet}$ toward most pollutants. Nevertheless, easily oxidized compounds such as anilines and sulphur-containing molecules can undergo significant degradation by $CO_3^{-\bullet}$ [4,11].

The excited triplet states of CDOM, ^{3}CDOM*, are formed upon radiation absorption by CDOM followed by inter-system crossing. They are quite powerful oxidizing species and play for instance a major role in the photoinduced degradation of phenylurea herbicides and sulphonamide antibiotics [12]. It has recently been found that phenolic antioxidants present in DOM may inhibit degradation reactions induced by ^{3}CDOM*. While it is highly unlikely that DOM significantly scavenges ^{3}CDOM*, these antioxidants could back-reduce, giving back the starting compounds, the pollutant molecules that have initially undergone oxidation upon reaction with ^{3}CDOM* [13].

Reaction between ^{3}CDOM* and O_2 produces singlet oxygen ($^1O_2$) that is also a reactive species. Reaction of $^1O_2$ with dissolved compounds (including organic pollutants) is in competition with the deactivation of $^1O_2$ upon collision with the solvent [3].

$$^3\text{CDOM}^* + O_2 \rightarrow \text{CDOM} + {}^1O_2 \quad (15)$$

$$^1O_2 \rightarrow O_2 \quad (16)$$

11.1.2. PHOTOTRANSFORMATION PROCESSES OF SOME PESTICIDE CLASSES

Pesticides constitute an extremely varied class of environmental contaminants and their fate, including photochemical transformation has, therefore, been the object of a huge number of studies. Here no attempt will be made to tackle the almost impossible task of providing a comprehensive review of the photochemical transformation processes of all known pesticides. On the contrary, examples of phototransformation reactions of some pesticides classes will be provided.

11.1.2.1. Phenoxyacetic acid herbicides

Chlorinated phenoxyacetic acid derivatives are extensively used for the protection of cereal crops against broad-leaf weeds. Examples are MCPA (4-chloro-2-methylphenoxyacetic acid), mecoprop ((RS)-2-(4-chloro-2-methylphenoxy)propanoic acid), 2,4-D (2,4-dichlorophenoxyacetic acid) and dichlorprop ((R)-2-(2,4-dichlorophenoxy)propanoic acid). Moreover, similar compounds bearing a trazole substituent on the alkyl chain are used as fungicides, including triadimefon ((RS)-1-(4-chlorophenoxy)-3,3-dimethyl-1-(1H-1,2,4-triazol-1-yl)butan-2-one) and triadimenol ((1RS,2RS;1RS,2SR)-1-(4-chlorophenoxy)-3,3-dimethyl-1-(1H-1,2,4-triazol-1-yl)butan-2-ol). The compounds used as herbicides are all characterised by the presence of a –COOH group, which is deprotonated under the pH conditions of surface waters. This is interesting, because the products of UV photolysis of the –COOH and -COO^- forms are quite different. The carboxylate forms can undergo photohydrolysis by replacement of the –Cl atom on the aromatic ring by a –OH group, while carboxylic acids mainly undergo a radical rearrangement *via* a solvent-cage process. This means that irradiation causes the break of a chemical bond that splits the molecule into two radicals, initially surrounded by the cage of water molecules. In such an environment, the radical-radical reaction is highly favoured and it can produce either the starting compounds or rearrangement products [14]. An example of the described reactions is provided for MCPA in Figure 11.2.

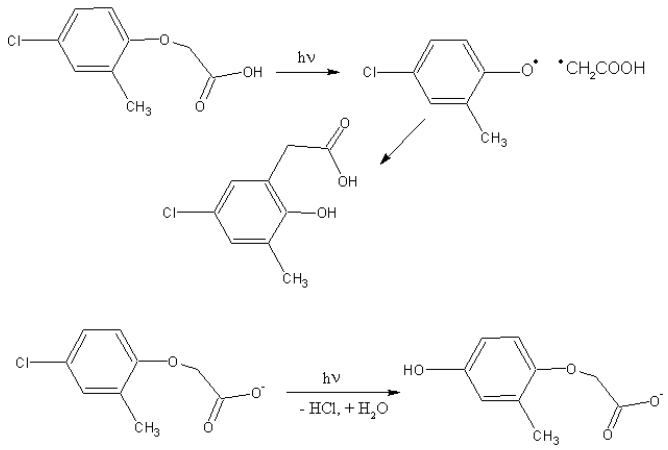

Figure 11.2. Direct photolysis processes of the protonated and deprotonated forms of MCPA.

An important finding is that irradiation of phenoxyacetic acid herbicides under sunlight also causes the loss of the acid chain to give the corresponding chlorophenol compounds: 2,4-chlorophenol from 2,4-D and from dichlorprop, 4-chloro-2-methylphenol from MCPA and from mecoprop. In a similar way, 4-chlorophenol (as well as 1,2,4-triazole) has been identified upon photolysis of mecoprop and triadimefon [14]. The 4-chloro-2-methylphenol accounts for the increase of toxicity of irradiated MCPA mixtures with irradiation time [14].

Interestingly, among the transformation intermediates of phenoxyacid herbicides, the cited chlorophenols have been found at the highest concentrations in the environment (but they are also impurities of the pesticide formulation, which adds to their environmental occurrence). In nitrate and nitrite-rich waters such as in flooded paddy fields, herbicide-derived chlorophenols can undergo efficient nitration reactions to produce toxic and potentially mutagenic nitroderivatives. Such compounds have actually been detected in waters of the Rhône delta (Southern France). The nitration process is mostly likely induced by $^{\bullet}NO_2$, produced by irradiation of nitrate and nitrite (reactions 1, 2, 13) [15-17].

11.1.2.2. Phenylurea herbicides

This class of herbicides includes compounds of rather widespread use such as monuron, metobromuron, diuron and linuron. Their direct photolysis has been shown to proceed mainly by photohydrolysis, *i.e.* the replacement of a halogen atom by a –OH group. Where applicable, the loss of a $-OCH_3$ group from the lateral alkyl chain (demethoxylation) may also take place [18]. Phenylurea herbicides have been shown to undergo transformation in surface waters mainly upon reaction with ^{3}CDOM* [12], but the detected intermediates are not much different from those of direct photolysis [12,18]. This similarity between intermediates of different photochemical pathways is not uncommon and it characterises other compounds as well [19]. Phenylureas are aniline analogues, and the electron couple on the N atom linked to the aromatic ring would increase the ring electron density. Therefore, these compounds are activated to electrophilic and similar processes, and nitration of phenylureas has for instance been observed under photochemical conditions in the presence of nitrate and nitrite as $^{\bullet}NO_2$ sources [20].

11.1.2.3. Halogenated phenol derivatives

Pesticides belonging to this miscellaneous class would mainly undergo transformation *via* photohydrolysis. This behaviour has been observed for instance with bromoxynil (3,5-dibromo-4-hydroxybenzonitrile) as well as its chlorinated and iodinated congeners [21], with dichlorophen (2,2'-methylenebis(4-chlorophenol)) [22] and partially with dicamba (3,6-dichloro-2-methoxybenzoic acid) [23]. In the latter case, the presence of a carboxylic group in *ortho* position to a methoxy one enables a cyclisation process that takes place along with photohydrolysis (Figure 11.3).

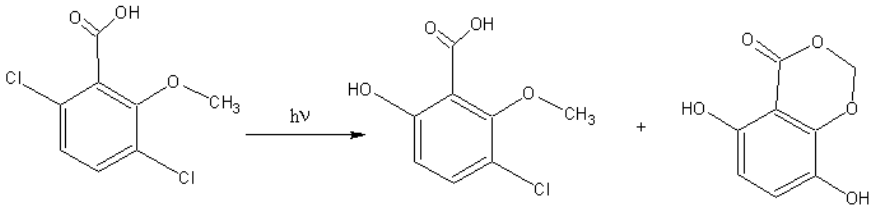

Figure 11.3. Direct photolysis of dicamba in aqueous solution.

Photohydrolysis has been detected (but only as a secondary process) in the case of acifluorfen (5-(2-chloro-α,α,α-trifluoro-p-tolyl)-2-nitrobenzoic acid), mainly because the nitrobenzoic acid ring is more reactive than the phenolic one. As a consequence, decarboxylation as well as breaking of the ether bond between the two rings have been observed as the main transformation pathways. Acifluorfen is probably unreactive with ^{3}CDOM*, but it has been found to undergo efficient degradation by $^\bullet$OH [24].

11.1.2.4. Atrazine and other triazines

In a study of the direct photolysis of the herbicide atrazine and of its reaction with $^\bullet$OH, transformation intermediates by both processes have been identified (they are listed in Table 11.1). The main intermediates of direct photolysis arise from photohydrolysis (replacement of the chlorine atom on the triazine ring with a –OH group) and from oxidation of the lateral alkyl chains. In contrast, no photohydrolysis was observed with $^\bullet$OH and, in addition to oxidation, complete cleavage of the lateral chains was detected. Interestingly, the compounds deriving from lateral-chain oxidation have been observed in both direct photolysis and $^\bullet$OH reaction [25], which is not uncommon as far as photochemical transformation pathways (direct or indirect) are concerned [19].

In the case of Irgarol 1051 (2-methylthio-4-tert-butylamino-6-cyclopropylamino-s-triazine), used in antifouling paints, the products of direct and CDOM-sensitised transformation were found to practically coincide. Transformation pathways included modification or cleavage of the lateral chains (dealkylation), oxidation of the methylthio group or its replacement with –OH [26].

Table 11.1. Main identified transformation intermediates of atrazine upon direct photolysis and reaction with •OH. N/a: not applicable. ☑: the compound was observed under the reported conditions.

Formula	Name	Photolysis	•OH
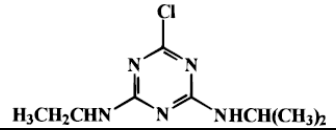	Atrazine (2-chloro-4-ethylamino-6-isopropylamino-s-triazine)	N/a	N/a
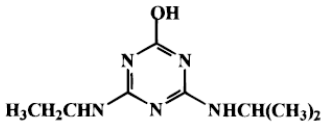	Hydroxyatrazine (4-ethylamino-2-hydroxy-6-isopropylamino-s-triazine)	☑	
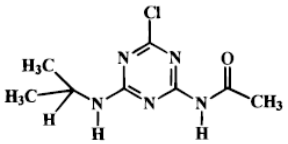	4-acetamido-2-chloro-6-isopropylamino-s-triazine	☑	☑
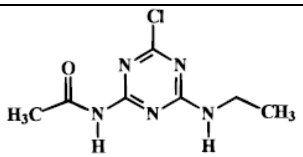	4-acetamido-2-chloro-6-ethylamino-s-triazine	☑	☑
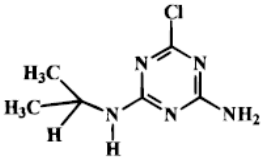	6-amino-2-chloro-4-isopropylamino-s-triazine		☑
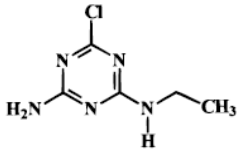	6-amino-2-chloro-4-ethylamino-s-triazine		☑

11.1.2.5. Propiconazole

The fungicide propiconazole (1-[2-(2,4-dichlorophenyl)-4-propyl-1,3-dioxolan-2-ylmethyl]-1H-1,2,4-triazole) has been found to undergo a cyclisation process upon photolysis, which gives a condensed three-ring structure upon elimination of HCl (Figure 11.4). Moreover, oxidation products have been detected upon irradiation in natural waters [27].

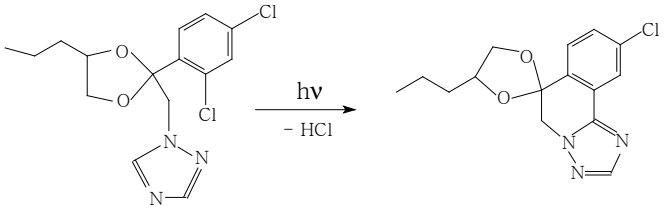

Figure 11.4. Photocyclisation of propiconazole.

11.1.2.6. Sulphur-containing compounds

The fungicide carboxin (5,6-dihydro-2-methyl-1,4-oxathi-ine-3-carboxanilide) undergoes photolysis by oxidation of the sulphur atom to a sulphoxide group. The reaction also proceeds by release of oxanilic acid. Oxidation of the sulphur atom can also take place upon reaction with singlet oxygen and other photoinduced oxidants, and it could play an important role in carboxin photolysis: for instance the related fungicide oxycarboxin (5,6-dihydro-2-methyl-1,4-oxathi-ine-3-carboxanilide-4,4-dioxide) bears a sulphone group that cannot be further oxidised, which may account for its much slower photodegradation compared to carboxin [28].

The herbicide florasulam (N-(2,6-difluorophenyl)-5-methoxy-8-fluoro(1,2,4)-triazolo-[1,5-c]-pyrimidine-2-sulphonamide) undergoes direct photolysis by release of the difluorophenyl group and production of a sulphonic acid derivative. However, indirect phototransformation of florasulam in natural waters is considerably faster than direct photolysis. The sensitised process proceeds by difluorophenyl release to form a sulphonamide, and/or by replacement with –OH of the methoxy group on the pyrimidine ring. Moreover, the pyrimidine moiety can be disrupted by leaving a carboxylic group linked to the triazole ring [29].

11.1.2.7. Carbamate insecticides

Carbofuran (2,3-dihydro-2,2-dimethyl-7-benzofuranyl-N-methylcarbamate) undergoes photoinduced cleavage of the carbamic moiety to give a phenolic derivative, followed by photohydrolysis of the furan ring to produce a catechol dervative (3-(2-hydroxy-sec-butyl)catechol) [30]. The photodegradation of carbofuran is inhibited by DOM, partially upon competition with CDOM for sunlight irradiance (which inhibits direct photolysis), and partly upon carbofuran-DOM interaction that inhibits phototransformation. The latter process might involve an enhancement of the thermal deactivation of carbofuran excited states, which would inhibit further chemical reactions [30].

The transformation of carbaryl is enhanced in natural waters compared to ultra-pure one, indicating that indirect photochemistry may be important in addition to direct photolysis. Reaction with $^{\bullet}OH$ and possibly with $^{3}CDOM^{*}$ and/or $^{1}O_2$ are reasonable candidate processes for indirect photochemistry [31].

11.2. PHOTOTRANSFORMATION OF PESTICIDES IN SOIL AND THE ATMOSPHERE

11.2.1. PHOTOCHEMICAL REACTIONS IN SOIL

Photodegradation of pesticides in soil is obviously limited by sunlight penetration, which is certainly more difficult below ground than below water. Anyway, photochemical processes would take place in the topmost soil layer that is often the first portion coming into contact with pesticides. Similarly to surface waters, photoreactions can be divided into direct and indirect photolysis. Direct photolysis on solid surfaces may be different than in solution, because of the absence of the cage of water molecules and, sometimes, for the directional effect of surfaces. The water-cage effect usually inhibits direct photolysis, because in the solution bulk the photofragments are initially surrounded by water molecules that make photofragment recombination easier (Figure 11.5) [32]. The photofragments often recombine to yield the parent compound, although photoisomerisation is also possible (see for instance Figure 11.2). Being a transformation process, cage photoisomerisation does not decrease the photolysis quantum yield. Generally speaking, it could be assumed that the photolysis quantum yields would often

be higher in soil than in water, which is counterbalanced by a lower availability of sunlight in soil. Moreover, processes such as photoisomerisation and photohydrolysis are more likely to take place in aqueous solution than on the soil surface.

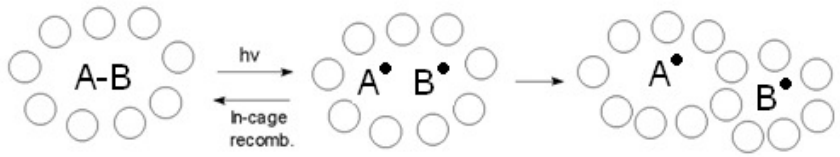

Figure 11.5. Schematic diagram of the solvent-cage effect for photochemical reactions in aqueous solution. Open circles represent solvent molecules.

Perhaps the most important difference between water and soil is related to sensitised phototransformation. In the case of soil surfaces, a significant fraction of indirect photochemistry would be triggered by photoactive minerals (most notably the semiconductor oxides) that do not play an important role in surface waters [33]. Examples include TiO_2, ZnO and Fe(III) (hydr)oxides. The photochemistry of the latter is perhaps more complex because it does not follow a pure semiconductor mechanism (*vide infra*) [34].

A mineral having semiconducting properties can be photoactive if its band-gap energy is comparable to the energy of sunlight photons. If this is the case, radiation absorption promotes an electron from the valence to the conduction band, leaving a hole (electron vacancy) in the valence band. Electron and holes can recombine producing heat, or they can migrate to the semiconductor surface where trapping by surface and sub-surface species is possible. Recombination between surface-trapped electrons and holes is still possible, but it is considerably slower than in the semiconductor bulk and enables chemical reactivity to take place. The conduction-band electron (e_{CB}^-) is a reductant and can, for instance, transform molecular oxygen into $O_2^{-\bullet}$. The valence-band hole (h_{VB}^+) is an oxidant and can oxidise compounds that are adsorbed on the semiconductor surface, including pesticide molecules (Figure 11.6).

In the case of the very-well known semiconducting oxide TiO_2, the holes of the valence band can be trapped by surface $\equiv Ti^{4+}\text{-}OH^-$ groups (producing $\equiv Ti^{4+}\text{-}{}^{\bullet}OH$, also called surface-adsorbed $^{\bullet}OH$) or sub-surface $\equiv Ti^{4+}\text{-}O^{2-}\text{-}Ti^{4+}\equiv$ species (yielding $\equiv Ti^{4+}\text{-}O^{\bullet-}\text{-}Ti^{4+}\equiv$, sub-surface holes) [35].

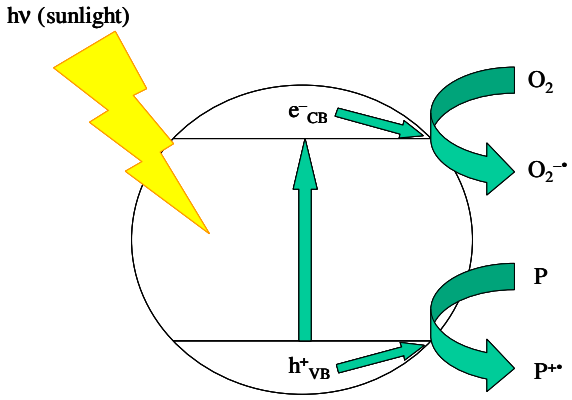

Figure 11.6. Processes following radiation absorption by a generic semiconductor oxide. P means pollutant (*e.g.* pesticide).

The species $\equiv Ti^{4+}$-$^{\bullet}OH$ has qualitatively similar (but quantitatively lower) reactivity as free $^{\bullet}OH$, while $\equiv Ti^{4+}$-$O^{\bullet-}$-$Ti^{4+}\equiv$ is mostly involved in electron-transfer processes with adsorbed substrates. Conduction-band e^- can be trapped by Ti^{4+} ions to give Ti^{3+}, also named surface-adsorbed electron. Very interestingly, the reductive pathways triggered by e_{CB}^- can produce oxidising species with the following reaction sequence [36] ($O_2^{-\bullet}$ is produced upon O_2 reduction by e_{CB}^-):

$$O_2^{-\bullet} + H^+ \leftrightarrows HO_2^{\bullet} \quad (17)$$
$$O_2^{-\bullet} + HO_2^{\bullet} + H^+ \rightarrow H_2O_2 + O_2 \quad (18)$$
$$H_2O_2 + h\nu \rightarrow 2\ ^{\bullet}OH \quad (19)$$
$$H_2O_2 + e_{CB}^- \rightarrow {}^{\bullet}OH + OH^- \quad (20)$$

Reactions (17)-(20) yield free $^{\bullet}OH$ in solution rather than surface-adsorbed species. Therefore, rather surprisingly, bulk $^{\bullet}OH$ in photocatalysis is produced by the reductant e_{CB}^- rather than by the oxidant h_{VB}^+ [37].

The semiconductor oxide ZnO has similar behaviour as TiO_2, although it has been subjected to many fewer studies. Both ZnO and TiO_2 are characterised by the absorption of sunlight only below 400 nm, thus only environmental UV radiation is available for the described reactions to take place [35].

Fe(III) (hydr)oxides absorb a considerably larger fraction of sunlight (typically, radiation absorption takes place below 550 nm), but this does not imply higher photoactivity compared with ZnO and TiO_2. In fact, despite easier production of e_{CB}^- and h_{VB}^+ in Fe(III) compounds, their recombination is much faster and considerably hampers photoactivity. Therefore, semiconductor-like photoactivity of Fe(III) (hydr)oxides is quite limited [34]. However, these compounds can also undergo photolysis of the surface $=Fe^{3+}$-OH^- groups upon absorption of UV radiation, yielding $^{\bullet}OH$ and Fe^{2+} that can further react with H_2O_2 to give additional $^{\bullet}OH$ (Fenton reaction) [38].

$$=Fe^{3+}\text{-}OH^- + h\nu \rightarrow Fe^{2+} + {}^{\bullet}OH \quad (21)$$
$$Fe^{2+} + H_2O_2 \rightarrow Fe^{3+} + {}^{\bullet}OH + OH^- \quad (22)$$

The humic fraction of soil could potentially be able to induce pesticide photodegradation *via* triplet-state reactivity [39]. Indeed, soil-derived humic and fulvic acids are the most photoactive CDOM components in surface waters and they are definitely more important in soil. Although the lower amount of water available might be unfavourable to such processes, *e.g.* by limiting solute transport [40], this is a potentially important process that has received comparatively little attention by now.

Another important issue is that pesticides can be photodegraded on the leaf surface, which is often the site of their first application. Reactions in the waxy leaf environment might be somewhat different than in water and, as far as direct photolysis is concerned, similar considerations may apply as already seen for topsoil. However, pesticide molecules located deep in the leaf wax could even experience a more important solvent-cage effect than in water, because of the much higher solvent viscosity. Photodegradation on the leaf surface has for instance been described for sulcotrione [41], mesotrione [42], bentazon, clopyralid, and triclopyr [43], nicosulfuron [44], chlorothalonil [45] and cycloxydim [46].

11.2.2. PHOTOCHEMICAL REACTIONS IN THE ATMOSPHERE

Photochemical processes in the atmosphere follow the usual classification of direct and indirect photolysis. They can take place in the gas phase, on the particle surface and in suspended water droplets, depending on the volatility and the water solubility of the relevant compounds. Compared to the bulk phase of surface waters, direct photolysis processes would be favoured in the gas phase, on the particle surface and at the air-water interface of droplets (but not in the droplet bulk), because of the absence of the solvent cage (see Figure 11.7 for the case of the air-water interface of droplets) [32].

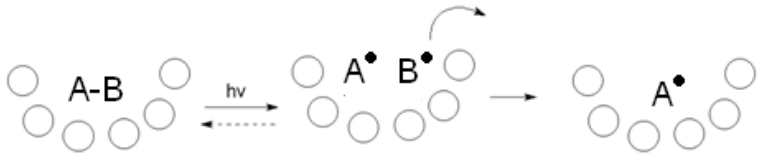

Figure 11.7. Direct photolysis process at the air-water interface (to be compared with Figure 11.5).

Enhanced interface photolysis would be operational in surface waters as well, but in that case the interface has a negligible weight compared to small droplets because of the unfavourable surface-to-volume ratio of large volumes. In the case of particles, direct photolysis can be inhibited by radiation screening effects. Indeed, black carbonaceous particles have been shown to protect adsorbed compounds against direct photolysis, mostly because of sunlight absorption [47].

As far as indirect photochemistry is concerned, the radical $^{\bullet}OH$ will certainly play a more important role in the atmospheric gas phase than in surface waters. The main reason for this is the efficient scavenging of $^{\bullet}OH$ by DOM in aqueous environments, which has no parallel in the atmospheric gas phase. In the latter case, $^{\bullet}OH$ reactivity is mainly a daylight one and it is triggered by the photolysis of several photoactive compounds: nitrous acid (HONO) in the early morning, formaldehyde later on and finally ozone at midday/afternoon [48]. The relevant processes are reported below.

$$HONO + h\nu \rightarrow {}^{\bullet}OH + {}^{\bullet}NO \quad (23)$$
$$HCHO + h\nu \rightarrow H^{\bullet} + CHO^{\bullet} \quad (24)$$
$$H^{\bullet} + O_2 \rightarrow HO_2^{\bullet} \quad (25)$$
$$HO_2^{\bullet} + {}^{\bullet}NO \rightarrow {}^{\bullet}OH + {}^{\bullet}NO_2 \quad (26)$$
$$O_3 + h\nu \rightarrow O_2 + O^* \quad (27)$$
$$O^* + H_2O \rightarrow 2\ {}^{\bullet}OH \quad (28)$$

The radical $^{\bullet}OH$ is mainly involved in electron-transfer processes (which are unlikely in the gas phase, however), hydrogen atom abstraction and addition to double bonds and aromatic rings [8]. The hydroxyl radical would essentially induce degradation processes during the day. Indeed, the combination of very high reactivity and of extremely low night-time production ensures that $^{\bullet}OH$ is almost absent from the atmosphere at night. Under such circumstances, gas-phase atmospheric reactivity is dominated by the nitrate radical ($^{\bullet}NO_3$), which is efficiently photolysed during the day but can survive in the absence of sunlight. The radical $^{\bullet}NO_3$ is produced by reaction between $^{\bullet}NO_2$ and ozone [48]:

$^{\bullet}NO_2 + O_3 \rightarrow {}^{\bullet}NO_3 + O_2$ (29)

Although less reactive than $^{\bullet}OH$, $^{\bullet}NO_3$ can reach higher concentration values in the atmosphere and can be important in the transformation of reactive pollutants and, most notably, of aromatic compounds. The radical $^{\bullet}NO_3$ can also abstract H atoms from aliphatics to produce HNO_3, but this process is considerably less efficient compared to $^{\bullet}OH$ reactions [48].

A further reactant in the atmospheric gas phase is O_3, but it is only important in the transformation of compounds having double C=C bonds. Ozone reactivity with *e.g.* aromatics or other organic compounds is very low to nil, in particular if compared with $^{\bullet}OH$ and $^{\bullet}NO_3$ [49].

In the case of particles, indirect photochemistry processes can be induced by irradiation of semiconductor oxides (see section 11.2.1) and of nitrate salts (most notably $NaNO_3$ and NH_4NO_3). In the latter case, production of $^{\bullet}OH$ is expected to take place in a similar way as in solution (see reaction 1) and it is enhanced in the presence of water vapour, which would most likely act as H^+ source [50]. In airborne particulate matter, transformation processes could also be induced by triplet sensitisers [51] such as quinones and aromatic carbonyls and by aromatic nitroderivatives (*e.g.* 1-nitronaphthalene. [52]). All these compounds are well known to efficiently produce triplet states under irradiation.

The photochemistry of atmospheric water droplets has many similarities but also important differences with surface-water photochemistry. First of all, due to the much higher surface-to-volume ratio, interface processes are definitely more important in droplets [32]. Moreover, chromophoric dissolved organic matter that is found in the atmospheric aqueous phase is considerably less reactive than surface-water CDOM. In other words, there is evidence that atmospheric humic-like substances (HULIS) may be considerably less reactive than surface-water humic and fulvic acids [53]. Furthermore, due to the more acidic pH of atmospheric *vs.* surface waters, processes involving Fe species (*e.g.* photolysis of $FeOH^{2+}$ and the Fenton reaction) would be more important in the atmospheric compartment (with minor exceptions such as acidic mine-drainage water) [54].

$FeOH^{2+} + h\nu \rightarrow Fe^{2+} + {}^{\bullet}OH$ (30)

In the case of surface waters, the very low concentration of hydrogen peroxide makes H_2O_2 a minor to negligible $^{\bullet}OH$ source under most circumstances. The situation is completely different in the atmospheric aqueous phase, where mass transfer from the gas phase makes H_2O_2 photolysis an important $^{\bullet}OH$ source [55,56]. However, differently from surface waters and again due to the much larger surface-to-volume ratio of atmospheric ones, $^{\bullet}OH$ transfer from the gas phase to the aqueous solution is usually the most important source of hydroxyl radical in atmospheric hydrometeors [57].

11.3. MODELLING PESTICIDES PHOTOTRANSFORMATION IN SURFACE WATERS

The model presented here describes the transformation kinetics of a substrate, a generic pollutant P, as a function of water chemistry and substrate reactivity, *via* the main photochemical reaction pathways that are operational in surface waters (direct photolysis and reaction with $^{\bullet}OH$, $CO_3^{-\bullet}$, $^1O_2$ and ^{3}CDOM*). It also calculates the steady-state concentrations of photogenerated transients in a cylindrical volume of 1 cm^2 surface area and depth *d*. The model may use actual data of water absorption spectrum or, in their absence, it can approximate the spectrum from the dissolved organic carbon (DOC) values. The DOC, in units of mg C L^{-1}, is a measure of DOM. The different aspects of the model are now described in greater detail.

11.3.1. SURFACE-WATER ABSORPTION SPECTRUM

It is possible to find a reasonable correlation between the absorption spectrum of surface waters and their content of dissolved organic matter, expressed as DOC. The following equation holds for the water spectrum, referred to an optical path length of 1 cm [58]:

$$A_1(\lambda) = (0.45 \pm 0.04) \cdot DOC \cdot e^{-(0.015 \pm 0.002)\lambda} \quad (31)$$

As an obvious alternative, $A_1(\lambda)$ can be spectrophotometrically determined on a real water sample.

11.3.2. REACTION WITH $^{\bullet}$OH [58]

In natural surface waters under sunlight illumination, the main $^{\bullet}$OH sources are (in order of average importance) Chromophoric Dissolved Organic Matter (CDOM), nitrite, and nitrate. All these species produce $^{\bullet}$OH upon absorption of sunlight. The calculation of the photon fluxes absorbed by CDOM, nitrate and nitrite requires to take into account the mutual competition for sunlight irradiance. Actually, CDOM is the main radiation absorber in the 300-500 nm region where also nitrite and nitrate absorb radiation. At a given wavelength λ, the ratio of the photon flux densities absorbed by two different species is equal to the ratio of the respective absorbances. The same is also true for the ratio of the photon flux density absorbed by species to the total photon flux density absorbed by the solution, $p_a^{tot}(\lambda)$ [2]. Accordingly, the following equations hold for the different $^{\bullet}$OH sources (note that $A_1(\lambda)$ is the specific absorbance of the surface water layer over a 1 cm optical path length, in units of cm^{-1}; d is the water column depth in m; $A_{tot}(\lambda)$ the total absorbance of the water column, and $p°(\lambda)$ the spectrum of sunlight, also called the incident photon flux density):

$$A_{tot}(\lambda) = 100\, A_1(\lambda) \cdot d \quad (32)$$

$$A_{NO3-}(\lambda) = 100\, \varepsilon_{NO3-}(\lambda) \cdot d \cdot [NO_3^-] \quad (33)$$

$$A_{NO2-}(\lambda) = 100\, \varepsilon_{NO2-}(\lambda) \cdot d \cdot [NO_2^-] \quad (34)$$

$$A_{CDOM}(\lambda) = A_{tot}(\lambda) - A_{NO3-}(\lambda) - A_{NO2-}(\lambda) \approx A_{tot}(\lambda) \quad (35)$$

$$p_a^{tot}(\lambda) = p°(\lambda) \cdot (1 - 10^{-A_{tot}(\lambda)}) \quad (36)$$

$$p_a^{CDOM}(\lambda) = p_a^{tot}(\lambda) \cdot A_{CDOM}(\lambda) \cdot [A_{tot}(\lambda)]^{-1} \approx p_a^{tot}(\lambda) \quad (37)$$

$$p_a^{NO2-}(\lambda) = p_a^{tot}(\lambda) \cdot A_{NO2-}(\lambda) \cdot [A_{tot}(\lambda)]^{-1} \quad (38)$$

$$p_a^{NO3-}(\lambda) = p_a^{tot}(\lambda) \cdot A_{NO3-}(\lambda) \cdot [A_{tot}(\lambda)]^{-1} \quad (39)$$

An important issue is that $p°(\lambda)$ is usually reported in units of Einstein cm^{-2} s^{-1} nm^{-1} (see for instance Figure 11.8), thus the absorbed photon flux densities are expressed in the same units. To express the formation rates of $^{\bullet}$OH in M s^{-1}, the absorbed photon fluxes P_a^i should be expressed in Einstein L^{-1} s^{-1}. Integration of $p_a^i(\lambda)$ over wavelength would give units of Einstein cm^{-2} s^{-1} that represent the moles of photons absorbed per unit surface area and unit time.

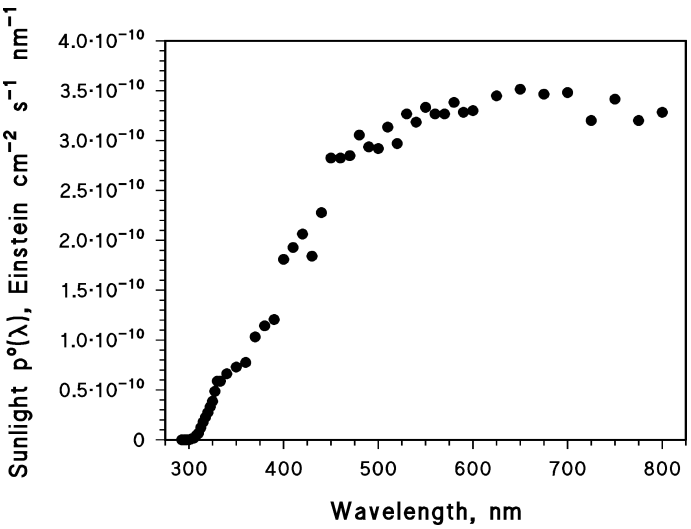

Figure 11.8. Sunlight spectral photon flux density at the water surface per unit area. The corresponding UV irradiance is 22 W m^{-2} [59].

Assuming a cylindrical volume of unit surface area (1 cm^2) and depth *d* (expressed in m), the absorbed photon fluxes in Einstein L^{-1} s^{-1} units would be expressed as follows (note that 1 L = 10^3 cm^3 and 1 m = 10^2 cm):

$$P_a^{CDOM} = 10\, d^{-1} \int_\lambda p_a^{CDOM}(\lambda)\, d\lambda \tag{40}$$

$$P_a^{NO2-} = 10\, d^{-1} \int_\lambda p_a^{NO2-}(\lambda)\, d\lambda \tag{41}$$

$$P_a^{NO3-} = 10\, d^{-1} \int_\lambda p_a^{NO3-}(\lambda)\, d\lambda \tag{42}$$

Various studies have yielded useful correlation between the formation rate of $^\bullet$OH by the photoactive species and the respective absorbed photon fluxes of sunlight. In particular, it has been found that [58,60]:

$$R_{^\bullet OH}^{CDOM} = (3.0 \pm 0.4) \cdot 10^{-5} \cdot P_a^{CDOM} \tag{43}$$

$$R_{^\bullet OH}^{NO2-} = \int_\lambda \Phi_{^\bullet OH}^{NO_2^-}(\lambda)\ \ p_a^{NO2-}(\lambda)\, d\lambda \tag{44}$$

$$R_{^\bullet OH}^{NO3-} = (4.3 \pm 0.2) \cdot 10^{-2} \cdot \frac{[IC] + 0.0075}{2.25\,[IC] + 0.0075} \cdot P_a^{NO3-} \tag{45}$$

where [IC] = $[H_2CO_3]$ + $[HCO_3^-]$ + $[CO_3^{2-}]$ is the total amount of inorganic carbon. The wavelength-dependent data of $\Phi_{^\bullet OH}^{NO_2^-}(\lambda)$ are reported in Table 11.2 [5].

Table 11.2. Values of the quantum yield of $^{\bullet}OH$ photoproduction by nitrite, for different wavelengths of environmental significance.

λ, nm	$\Phi_{^{\bullet}OH}^{NO_2^-}(\lambda)$	λ, nm	$\Phi_{^{\bullet}OH}^{NO_2^-}(\lambda)$	λ, nm	$\Phi_{^{\bullet}OH}^{NO_2^-}(\lambda)$
292.5	0.0680	315.0	0.061	350	0.025
295.0	0.0680	317.5	0.058	360	0.025
297.5	0.0680	320.0	0.054	370	0.025
300.0	0.0678	322.5	0.051	380	0.025
302.5	0.0674	325.0	0.047	390	0.025
305.0	0.0668	327.5	0.043	400	0.025
307.5	0.066	330.0	0.038	410	0.025
310.0	0.065	333.3	0.031	420	0.025
312.5	0.063	340.0	0.026	430	0.025

At the present state of knowledge it is reasonable to hypothesise that CDOM, nitrite and nitrate generate $^{\bullet}OH$ independently, with no mutual interactions. Therefore, the total formation rate of $^{\bullet}OH$ ($R_{^{\bullet}OH}^{tot}$) is the sum of the contributions of the three species:

$$R_{^{\bullet}OH}^{tot} = R_{^{\bullet}OH}^{CDOM} + R_{^{\bullet}OH}^{NO2-} + R_{^{\bullet}OH}^{NO3-} \qquad (46)$$

Accordingly, having as input data d, $A_1(\lambda)$, $[NO_3^-]$, $[NO_2^-]$ and $p°(\lambda)$ (the latter referred to a 22 W m^{-2} sunlight UV irradiance, see Figure 11.8), it is possible to model the expected $R_{^{\bullet}OH}^{tot}$ of the sample. The photogenerated $^{\bullet}OH$ radicals could react either with the pollutant P or with the natural scavengers present in surface water (mainly organic matter, bicarbonate, carbonate and nitrite). The natural scavengers have the following $^{\bullet}OH$ scavenging rate constant:
$\Sigma_i k_{Si} [S_i] = 5\times10^4\ DOC + 8.5\times10^6\ [HCO_3^-] + 3.9\times10^8\ [CO_3^{2-}] + 1.0\times10^{10}\ [NO_2^-]$ (units of s^{-1}; DOC is expressed in mg C L^{-1} and the other concentration values are in molarity). Accordingly, the reaction rate between P and $^{\bullet}OH$ can be expressed as follows:

$$R_P^{^{\bullet}OH} = R_{^{\bullet}OH}^{tot} \frac{k_{P,^{\bullet}OH}[P]}{k_{P,^{\bullet}OH}[P] + \sum_i k_{Si}[S_i]} \qquad (47)$$

where $k_{P,^{\bullet}OH}$ is the second-order reaction rate constant between P and $^{\bullet}OH$ and [P] is a molar concentration. Note that, in the vast majority of environmental cases it would be $k_{P,^{\bullet}OH}[P] \ll \Sigma_i k_{Si}[S_i]$, thus the $k_{P,^{\bullet}OH}[P]$ term can be neglected at the denominator of equation (47). The pseudo-first order degradation rate constant of P is $k_P = R_{^{\bullet}OH}^{P}[P]^{-1}$, and the half-life time is $t_P = \ln 2\ k_P^{-1}$. The time t_P is expressed in seconds of continuous irradiation under sunlight, at 22 W m^{-2} UV irradiance (see Figure 11.8 for the sunlight spectrum). It has been shown that the sunlight energy reaching the ground in a summer sunny day (SSD) such as 15 July at 45°N latitude corresponds to 10 h = $3.6\cdot10^4$ s of continuous irradiation at 22 W m^{-2} UV irradiance [61]. Accordingly the half-life time of P, because of reaction with $^{\bullet}OH$, would be expressed as follows in SSD units:

$$\tau_{P,^{\bullet}OH}^{SSD} = \frac{\ln 2 \sum_i k_{Si}[S_i]}{3.6\cdot10^4\ R_{^{\bullet}OH}^{tot}\ k_{P,^{\bullet}OH}} = 1.9\cdot10^{-5} \frac{\sum_i k_{Si}[S_i]}{R_{^{\bullet}OH}^{tot}\ k_{P,^{\bullet}OH}} \qquad (48)$$

Note that $1.9\cdot10^{-5} = \ln 2\ (3.6\cdot10^4)^{-1}$. The steady-state [$^{\bullet}OH$] under 22 W m^{-2} UV irradiance would be:

$$[^{\bullet}OH] = \frac{R_{^{\bullet}OH}^{tot}}{\sum_i k_{Si}\,[S_i]} \qquad (49)$$

11.3.3. DIRECT PHOTOLYSIS [62,63]

The calculation of the photon flux absorbed by P requires taking into account the mutual competition for sunlight irradiance between P and the other water components (mostly Chromophoric Dissolved Organic Matter, CDOM, which is the main sunlight absorber in the spectral region of interest, around 300-500 nm).

Under the Lambert-Beer approximation, at a given wavelength λ, the ratio of the photon flux densities absorbed by two different species is equal to the ratio of the respective absorbances [2]. Accordingly, the photon flux absorbed by P in a water column of depth d (expressed in m) can be obtained as follows (note that $A_1(\lambda)$ is the specific absorbance of the surface water sample over a 1 cm optical path length, $A_{tot}(\lambda)$ the total absorbance of the water column, $p°(\lambda)$ the spectrum of sunlight, referred to a UV irradiance of 22 W m^{-2} as per Figure 11.8, $\varepsilon_P(\lambda)$ the molar absorption coefficient of P, in units of M^{-1} cm^{-1}, and $p_a^P(\lambda)$ its absorbed spectral photon flux density; it is also $p_a^P(\lambda) \ll p_a^{tot}(\lambda)$ and $A_P(\lambda) \ll A_{tot}(\lambda)$ in the very vast majority of the environmental cases):

$$A_{tot}(\lambda) = 100\, A_1(\lambda) \cdot d \qquad (50)$$

$$A_P(\lambda) = 100\, \varepsilon_P(\lambda) \cdot d \cdot [P] \qquad (51)$$

$$p_a^{tot}(\lambda) = p°(\lambda) \cdot (1 - 10^{-A_{tot}(\lambda)}) \qquad (52)$$

$$p_a^P(\lambda) = p_a^{tot}(\lambda) \cdot A_P(\lambda) \cdot [A_{tot}(\lambda)]^{-1} \qquad (53)$$

To express the rate of P photolysis in M s^{-1}, the absorbed photon flux P_a^P should be expressed in Einstein L^{-1} s^{-1}. Integration of $p_a^P(\lambda)$ over wavelength gives units of Einstein cm^{-2} s^{-1} that represent the moles of photons absorbed per unit surface area and unit time. Assuming a cylindrical volume of unit surface area (1 cm^2) and depth d (expressed in m), the absorbed photon flux in Einstein L^{-1} s^{-1} units would be expressed as follows (note that 1 L = 10^3 cm^3 and 1 m = 10^2 cm):

$$P_a^P = 10\, d^{-1} \int_\lambda p_a^P(\lambda)\, d\lambda \qquad (54)$$

The rate of photolysis of P, expressed in M s^{-1}, is (note that 1 L = 10^3 cm^3 and 1 m = 10^2 cm):

$$Rate_P = 10\, d^{-1} \int_\lambda \Phi_P(\lambda)\; p_a^P(\lambda)\, d\lambda \qquad (55)$$

where $\Phi_P(\lambda)$ is the photolysis quantum yield of P in the relevant wavelength interval, and d is expressed in cm (also note that 1 L = 10^3 cm^3). If only a single average value for Φ_P is known, it can be brought out of the integral as a constant. The pseudo-first order degradation rate constant of P is $k_P = Rate_P\,[P]^{-1}$, which corresponds to a half-life time $t_P = ln\ 2\ (k_P)^{-1}$. The time t_P is expressed in seconds of continuous irradiation under sunlight, at 22 W m^{-2} UV irradiance. The sunlight energy reaching the ground in a summer sunny day (SSD) such as 15 July at 45°N latitude corresponds to 10 h = 3.6·10^4 s continuous irradiation at 22 W m^{-2} UV irradiance [61]. Accordingly, the half-life time expressed in SSD units would be given by (note that $V = 0.1\ d$):

$$\tau^{SSD}_P = (3.6{\cdot}10^4)^{-1}\ ln\ 2\ (k_P)^{-1} = 1.9{\cdot\cdot}10^{-5}\ [P]\ (Rate_P)^{-1} =$$

$$= 1.9\cdot10^{-5}\,[P]\,V\left(\int_{\lambda}\Phi_P(\lambda)\;p_a^P(\lambda)\,d\lambda\right)^{-1} =$$

$$= \quad 1.9\cdot10^{-5} \quad [P] \quad V \quad \left(\int_{\lambda}\Phi_P(\lambda)\cdot p_a^{tot}(\lambda)\cdot A_P(\lambda)\cdot[A_{tot}(\lambda)]^{-1}\,d\lambda\right)^{-1} \quad =$$

$$= \frac{1.9\cdot10^{-5}\;V\;\;[P]}{\int_{\lambda}\Phi_P(\lambda)\;p°(\lambda)\;(1-10^{-100\;A_1(\lambda)\;d})\;\dfrac{\varepsilon_P(\lambda)}{A_1(\lambda)}\,d\lambda} \qquad (56)$$

Note that $1.9\cdot10^{-5} = (\ln 2)\,(3.6\cdot10^{4})^{-1}$.

11.3.4. REACTION WITH $CO_3^{-\bullet}$ [64]

The radical $CO_3^{-\bullet}$ can be produced upon oxidation of carbonate and bicarbonate by $^{\bullet}OH$, upon carbonate oxidation by $^3CDOM^*$, and possibly also from irradiated Fe(III) oxide colloids and carbonate. However, as far as the latter process is concerned, there is still insufficient knowledge about the Fe speciation in surface waters to enable a proper modelling. The main sink of the carbonate radical in surface waters is the reaction with DOM, which is considerably slower than that between DOM and $^{\bullet}OH$.

$^{\bullet}OH + CO_3^{2-} \rightarrow OH^- + CO_3^{-\bullet}$	$[k_{27} = 3.9\times10^8\ M^{-1}\ s^{-1}]$	(57)
$^{\bullet}OH + HCO_3^- \rightarrow H_2O + CO_3^{-\bullet}$	$[k_{28} = 8.5\times10^6\ M^{-1}\ s^{-1}]$	(58)
$^3CDOM^* + CO_3^{2-} \rightarrow CDOM^{-\bullet} + CO_3^{-\bullet}$	$[k_{29} \approx 1\times10^5\ M^{-1}\ s^{-1}]$	(59)
$DOM + CO_3^{-\bullet} \rightarrow DOM^{+\bullet} + CO_3^{2-}$	$[k_{30} \approx 10^2\ (mg\ C)^{-1}\ s^{-1}]$	(60)

The formation rate of $CO_3^{-\bullet}$ in reactions (57, 58) is given by the formation rate of $^{\bullet}OH$ times the fraction of $^{\bullet}OH$ that reacts with carbonate and bicarbonate, as follows:

$$R_{CO_3^{-\bullet}}^{{}^{\bullet}OH} = R_{{}^{\bullet}OH}^{tot}\cdot\frac{8.5\cdot10^6\cdot[HCO_3^-]+3.9\cdot10^8\cdot[CO_3^{2-}]}{5\cdot10^4\cdot DOC+1.0\cdot10^{10}\cdot[NO_2^-]+8.5\cdot10^6\cdot[HCO_3^-]+3.9\cdot10^8\cdot[CO_3^{2-}]} \qquad (61)$$

The formation of $CO_3^{-\bullet}$ in reaction (59) is given by:

$$R_{CO_3^{-\bullet}}^{CDOM} = 6.5\cdot10^{-3}\cdot[CO_3^{2-}]\cdot P_a^{CDOM} \qquad (62)$$

The total formation rate of $CO_3^{-\bullet}$ is $R_{CO_3^{-\bullet}}^{tot} = R_{CO_3^{-\bullet}}^{{}^{\bullet}OH} + R_{CO_3^{-\bullet}}^{CDOM}$. The transformation rate of P by $CO_3^{-\bullet}$ is given by the fraction of $CO_3^{-\bullet}$ that reacts with P, in competition with reaction (30) between $CO_3^{-\bullet}$ and DOM:

$$R_{P,CO_3^{-\bullet}} = \frac{R_{CO_3^{-\bullet}}^{tot}\cdot k_{P,CO_3^{-\bullet}}\cdot[P]}{k_{30}\cdot DOC + k_{P,CO_3^{-\bullet}}\cdot[P]} \qquad (63)$$

where $k_{P,CO_3^{-\bullet}}$ is the second-order reaction rate constant between P and $CO_3^{-\bullet}$. In the very vast majority of the environmental cases it is $k_{P,CO_3^{-\bullet}}\,[P] \ll k_{30}\,DOC$.

In a pseudo-first order approximation, the rate constant of P transformation is $k_P = R_{P,CO_3^{\bullet-}} \cdot [P]^{-1}$ and the half-life time is $t_P = ln\ 2\ k_P^{-1}$. Considering the usual conversion (≈ 10 h) between a constant 22 W m^{-2} sunlight UV irradiance and a SSD unit, the following expression for $\tau_{NCP,CO3-\bullet}^{SSD}$ is obtained:

$$\tau_{P,CO_3^{\bullet-}}^{SSD} = 1.9 \cdot 10^{-5} \cdot \left(\frac{k_{30} \cdot DOC}{R_{CO_3^{\bullet-}}^{tot} \cdot k_{P,CO_3^{\bullet-}}} \right) \quad (64)$$

Note that $1.9 \cdot 10^{-5} = \ln 2\ (3.6 \cdot 10^4)^{-1}$. The steady-state $[CO_3^{\bullet-}]$ under 22 W m^{-2} UV irradiance would be:

$$[CO_3^{\bullet-}] = \frac{R_{CO_3^{\bullet-}}^{tot}}{k_{30} \cdot DOC} \quad (65)$$

11.3.5. REACTION WITH $^1O_2$ [65]

The formation of singlet oxygen in surface waters arises from energy transfer between ground-state molecular oxygen and the excited triplet states of CDOM (^{3}CDOM*). Accordingly, irradiated CDOM is practically the only source of $^1O_2$ in aquatic systems. In contrast, the main $^1O_2$ sink is the energy loss to ground-state O_2 by collision with water molecules, with a pseudo-first order rate constant $k_{^1O_2} = 2.5 \times 10^5$ s^{-1}. Dissolved species, including dissolved organic matter that is certainly able to react with $^1O_2$ would play a minor role as sinks of $^1O_2$ in aquatic systems. The main processes involving $^1O_2$ and P in surface waters would be the following:

$$^3CDOM^* + O_2 \rightarrow CDOM + {}^1O_2 \quad (66)$$

$$^1O_2 + H_2O \rightarrow O_2 + H_2O + heat \quad (67)$$

$$^1O_2 + P \rightarrow Products \quad (68)$$

In the Rhône delta waters it has been found that the formation rate of $^1O_2$ by CDOM is $R_{^1O_2}^{CDOM} = 1.25 \cdot 10^{-3}\ P_a^{CDOM}$ [66]. Considering the competition between the deactivation of $^1O_2$ by collision with the solvent (reaction 67) and reaction (68) with P, one gets the following expression for the degradation rate of P by $^1O_2$ (note that $k_{P,^1O_2} \cdot [P] \ll k_{^1O_2}$):

$$R_P^{^1O_2} = R_{^1O_2}^{CDOM} \cdot \frac{k_{P,^1O_2} \cdot [P]}{k_{^1O_2}} \quad (69)$$

In a pseudo-first order approximation, the rate constant of P transformation is $k_P = R_P^{^1O_2}\ [P]^{-1}$ and the half-life time is $t_P = ln\ 2\ k_P^{-1}$. Considering the usual conversion (≈ 10 h) between a constant 22 W m^{-2} sunlight UV irradiance and a SSD unit, the following expression for $\tau_{P,^1O_2}^{SSD}$ is obtained (remembering that $R_{^1O_2}^{CDOM} = 1.25 \cdot 10^{-3}\ P_a^{CDOM}$ and that $P_a^{CDOM} = 10^3\ d^{-1} \int_\lambda p_a^{CDOM}(\lambda)\, d\lambda$):

$$\tau_{P,^1O_2}^{SSD} = \frac{4.81}{R_{^1O_2}^{CDOM}\ k_{P,^1O_2}} = \frac{3.85 \cdot d}{k_{P,^1O_2} \cdot \int_\lambda p_a^{CDOM}(\lambda)\, d\lambda} \quad (70)$$

Note that 3.85 = (ln 2) k_{1O2} $(1.25 \cdot 10^{-3} \cdot 3.60 \cdot 10^{4} \cdot 10^{3})^{-1}$. The steady-state $[^1O_2]$ under 22 W m^{-2} UV irradiance would be:

$$[^1O_2] = \frac{R^{CDOM}_{^1O_2}}{k_{^1O_2}} \tag{71}$$

11.3.6. REACTION WITH ^{3}CDOM* [66]

The formation of excited triplet states of CDOM (^{3}CDOM*) in surface waters is a direct consequence of radiation absorption by CDOM. In aerated solution, ^{3}CDOM* could undergo thermal deactivation or reaction with O_2, and a pseudo-first order quenching rate constant $k_{^3CDOM^*} \approx 5 \cdot 10^5$ s^{-1} has been observed. The quenching of ^{3}CDOM* would be in competition with the reaction between ^{3}CDOM* and P:

$$\text{CDOM} + h\nu \rightarrow {}^3\text{CDOM}^* \tag{72}$$

$$^3\text{CDOM}^* \text{—(O}_2\text{)}\rightarrow \text{Deactivation and } ^1\text{O}_2 \text{ production} \tag{73}$$

$$^3\text{CDOM}^* + \text{P} \rightarrow \text{Products} \tag{74}$$

In the Rhône delta waters it has been found that the formation rate of ^{3}CDOM* is $R_{^3CDOM^*} = 1.28 \cdot 10^{-3}$ P_a^{CDOM} [66]. Considering the competition between reaction (74) with P and other processes (reaction 73), the following expression for the degradation rate of P by ^{3}CDOM* is obtained (note that $k_{P,^3CDOM^*} \cdot [P] \ll k_{^3CDOM^*}$, where $k_{P,^3CDOM^*}$ is the second-order reaction rate constant between P and ^{3}CDOM*):

$$R_P^{^3CDOM^*} = R_{^3CDOM^*} \cdot \frac{k_{P,^3CDOM^*} \cdot [P]}{k_{^3CDOM^*}} \tag{75}$$

In a pseudo-first order approximation, the rate constant of P transformation is $k_P = R_P^{^3CDOM^*} [P]^{-1}$ and the half-life time is $t_P = ln\ 2\ k_P^{-1}$. Considering the usual conversion (≈ 10 h) between a constant 22 W m^{-2} sunlight UV irradiance and a SSD unit, one gets the following expression for $\tau^{SSD}_{P,^3CDOM^*}$ (remembering that $P_a^{CDOM} = 10^3\ d^{-1} \int_\lambda p_a^{CDOM}(\lambda)\, d\lambda$):

$$\tau^{SSD}_{P,^3CDOM^*} = \frac{7.52 \cdot d}{k_{P,^3CDOM^*} \cdot \int_\lambda p_a^{CDOM}(\lambda)\, d\lambda} \tag{76}$$

Note that 7.52 = (ln 2) $k_{^3CDOM^*}$ $(1.28 \cdot 10^{-3} \cdot 3.60 \cdot 10^{4} \cdot 10^{3})^{-1}$. The steady-state $[^3CDOM^*]$ under 22 W m^{-2} UV irradiance would be:

$$[^3CDOM^*] = \frac{R_{^3CDOM^*}}{k_{^3CDOM^*}} \tag{77}$$

11.3.7. FORMATION OF INTERMEDIATES [19]

In the photochemical process *ph* (direct photolysis or reaction with $^{\bullet}OH$, $^{1}O_2$, $CO_3^{-\bullet}$, $^{3}CDOM^*$), the pollutant P could produce the intermediate I with yield y_I^{ph}, experimentally determined as the ratio between the initial formation rate of I and the initial transformation rate of P. The pseudo-first order rate constant of I formation in the process *ph* is $(k_I^{ph})' = y_I^{ph} k_P^{ph}$, where k_P^{ph} is the (model-derived) first-order transformation rate constant of P in the process *ph*. The production of I from P often takes place *via* more than one process. Therefore, the overall rate constant of I formation is:

$$(k_I)' = \sum_{ph} (k_I^{ph})' = \sum_{ph} (y_I^{ph} k_I^{ph}) \qquad (78)$$

One can also obtain the overall yield of I formation from P (y_I), as:

$$y_i = (k_I)'(k_P)^{-1} = \frac{\sum_{ph} (y_I^{ph} k_I^{ph})}{\sum_{ph} k_P^{ph}} \qquad (79)$$

11.3.8. THE MEANING OF WATER DEPTH IN THE MODEL

An important issue is that the model was not designed to make depth profiles of the transformation kinetics or of the concentration of reactive transients. Therefore, when setting depth as a variable, one actually compares different water bodies, each with its own depth value. This means that for, *e.g.*, 1 m depth the model returns the average [$^{\bullet}OH$] (or the steady-state concentration of other species) in the first 1 m of the water column. It should be underlined that it is the average concentration in the first 1 m of the column and not the point concentration at 1 m. One can also obtain the transformation kinetics of dissolved species in the hypothesis of thorough mixing in the water column, because the model applies to well-mixed shallow waters or to the top mixing layer of stratified water bodies. A key issue is that, if one wants to determine the photochemical reaction kinetics due to *e.g.* reaction with $^{\bullet}OH$ in the first 1 m of the water column, the needed value is the average [$^{\bullet}OH$] value (as determined by the model) and not the point [$^{\bullet}OH$] at 1 m.

11.3.9. MAIN APPROXIMATIONS OF THE MODEL

Surface waters represent an extremely complex and varied series of environments and the present attempt to describe their photochemical behaviour had to include a number of assumptions and approximations. The main ones are listed below.

- The model considers well-mixed water. Therefore, it applies to shallow water environments and to the well-mixed epilimnion of stratified ones.
- The Lambert-Beer approximation does not take radiation scattering into account. Therefore, the model applies to clear waters rather than to highly turbid ones.
- The data on which the modelling of surface-water absorption spectrum is based (equation 31) were obtained for lake water in NW Italy. There is evidence that applicability is much wider, but

more accurate results for a particular environment can be obtained if the actual water spectrum is available.

- The quantum yields for the formation of $^{\bullet}OH$ by CDOM are average values for NW Italian lakes. The corresponding data of $^1O_2$ and $^3CDOM^*$ have been obtained in the Rhône delta (S. France), and the value of $CO_3^{-\bullet}$ formation from $^3CDOM^*$ is from Lake Greifensee (Switzerland). In different environments, different values may be found. The best scenario is obviously attained when one has actual data measured in the water environment under study.
- The scavenging rate constants of $^{\bullet}OH$ and $CO_3^{-\bullet}$ by DOM are average values from the literature. The same consideration as above also applies here.

11.3.10. MODEL APPLICATION TO THE HERBICIDE MCPA

MCPA (4-chloro-2-methylphenoxyacetic acid) is a phenoxyacetic acid herbicide that undergoes photochemical transformation in the environment by direct photolysis and reaction with $^{\bullet}OH$ [67,68]. The main phototransformation intermediate is the toxic 4-chloro-2-methylphenol (CMP), which is formed from the parent compound by the two photochemical processes with different yields (0.3 for the direct photolysis and 0.5 for $^{\bullet}OH$). MCPA has a second-order reaction rate constant with $^{\bullet}OH$ of $6.6 \cdot 10^9$ M^{-1} s^{-1} [69], while the photolysis quantum yield depends on the DOC content of the solution. The main reason for this is that MCPA photolysis proceeds through reactions of its triplet state, which can be reduced to the radical anion (and the radical anion recycled back to initial MCPA by O_2) in the presence of dissolved organic compounds (S). The whole reaction set is as follows [68]:

$$MCPA + h\nu \rightarrow {}^1MCPA^* \text{—(ISC)}\rightarrow {}^3MCPA^* \quad (80)$$

$$^3MCPA^* + S \rightarrow MCPA^{-\bullet} + S^{+\bullet} \quad (81)$$

$$MCPA^{-\bullet} + O_2 \rightarrow MCPA + O_2^{-\bullet} \quad (82)$$

Therefore, the photolysis quantum yield of MCPA decreases with increasing DOC. An experimental assessment of the trend of Φ_{MCPA} *vs.* DOC gave the following results [68]:

$$\Phi_{MCPA} = \frac{(2.3 \pm 0.7) \cdot 10^{-5} + (4.3 \pm 0.1) \cdot 10^{-6}\, DOC}{(4.1 \pm 1.3) \cdot 10^{-5} + 1.4 \cdot 10^{-5}\, DOC} \quad (83)$$

With the above values for the $^{\bullet}OH$ reaction rate constant and the photolysis quantum yield, it is possible to model the half-life time of MCPA and the yield of CMP from MCPA, as a function of the chemical composition and depth of surface waters. Figure 11.9 reports the half-life time of MCPA (units of summer sunny days, SSD) as a function of depth and DOC (**a**) and as a function of nitrate and DOC (**b**). Figure 11.10 reports the yield η_{CMP} under the same conditions as for the previous figure (**a** and **b**).

Figure 11.9(a) shows that the modelled half-life time of MCPA (in the order of days to some months) increases with increasing DOC and depth. The increase with DOC is accounted for by the fact that CDOM and DOM are more concentrated at elevated DOC. CDOM inhibits MCPA direct photolysis by competing for sunlight irradiance, while DOM decreases the photolysis quantum yield (equation 83) and scavenges $^{\bullet}OH$. The increase of the half-life time with depth is due to the fact that the bottom layers of a deeper water body are less illuminated by sunlight, which does not favour the light-induced processes.

Figure 11.9(b) shows that, in addition to increasing with increasing DOC, the half-life time decreases with increasing nitrate that is a $^{\bullet}OH$ source and enhances MCPA transformation.

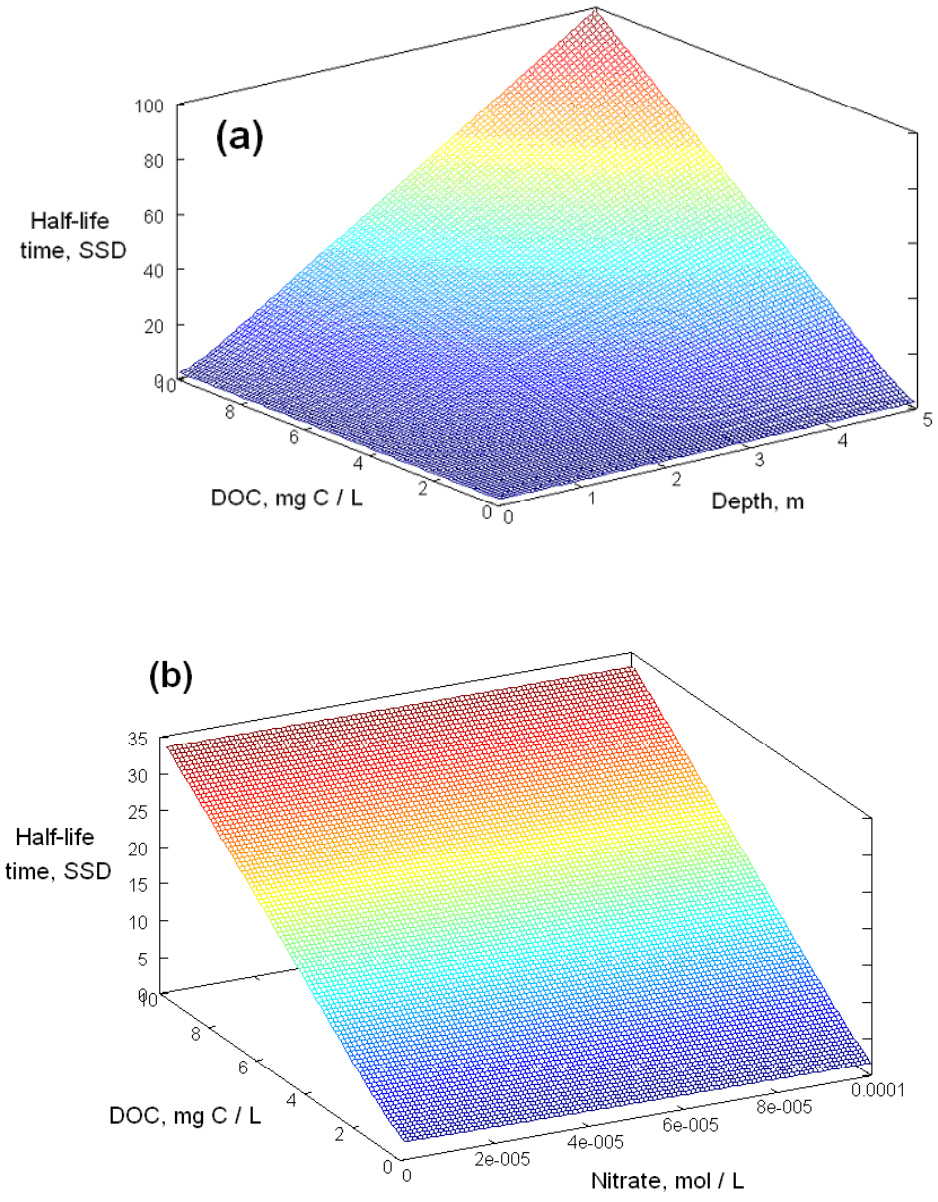

Figure 11.9. Modelled half-life time (SSD) of MCPA as a function of **(a)** DOC and depth (other water parameters: 1 µM nitrate, 10 nM nitrite, 2 mM bicarbonate, 10 µM carbonate), and **(b)** DOC and nitrate (other water parameters: 2 m depth, 10 nM nitrite, 2 mM bicarbonate, 10 µM carbonate).

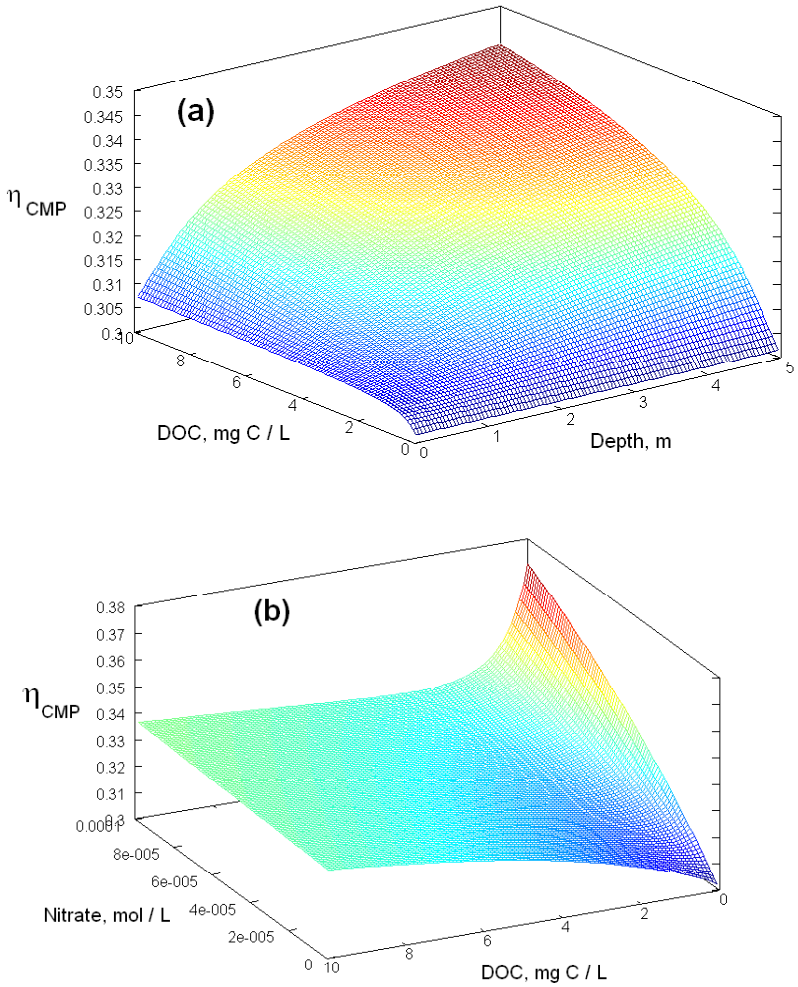

Figure 11.10. Modelled CMP yield from MCPA, as a function of **(a)** DOC and depth (other water parameters: 1 µM nitrate, 10 nM nitrite, 2 mM bicarbonate, 10 µM carbonate), and **(b)** DOC and nitrate (2 m depth, 10 nM nitrite, 2 mM bicarbonate, 10 µM carbonate).

Figure 11.10(a) shows that the yield of CMP from MCPA increases with depth and DOC, which both favour $^{\bullet}$OH reactions over the direct photolysis (remember that the $^{\bullet}$OH yield, 0.5, is higher than the yield by direct photolysis, 0.3). The reason is that MCPA mainly absorbs UVB radiation, which has poor penetration inside the water body. In contrast, the $^{\bullet}$OH sources CDOM and nitrite also absorb significantly in the UVA region (and CDOM absorbs in the visible as well).

Figure 11.10(b) shows that the yield increases with increasing nitrate as $^{\bullet}$OH source (which obviously enhances degradation by $^{\bullet}$OH) and that it has an interesting trend with DOC. At low nitrate the yield increases with increasing DOC because, under such conditions, CDOM is the main $^{\bullet}$OH source and $^{\bullet}$OH formation by CDOM offsets $^{\bullet}$OH scavenging by DOM. At high nitrate the trend of η_{CMP} *vs.* DOC has a minimum, because the initial increase of DOC has the main effect of scavenging the $^{\bullet}$OH radicals produced by nitrate, thereby inhibiting the $^{\bullet}$OH+MCPA reaction more than it inhibits direct photolysis. At high DOC, CDOM becomes the main $^{\bullet}$OH source and an increase of DOC inhibits MCPA direct photolysis (through competition between CDOM and MCPA for irradiance and because DOM decreases the photolysis quantum yield) to a higher extent than it inhibits $^{\bullet}$OH reactions.

REFERENCES

1. Wayne, R.P., Basic concepts of photochemical transformations. In: Boule, P., Bahnemann, D.W., Robertson, P. K. J. (Eds.), *The Handbook of Environmental Chemistry Vol. 2.M – Environmental Photochemistry Part II*, Springer, Berlin, 2005, pp. 1-47.
2. Braslavsky, S.E., Glossary of terms used in photochemistry, 3rd edition, *Pure Appl. Chem.*, 79, 293-465, 2007.
3. Boreen, A.L., Arnold, W.A., and McNeill, K., Photodegradation of pharmaceuticals in the aquatic environment: A review. *Aquat. Sci.*, 65, 320-341, 2003.
4. Canonica, S., Kohn, T., Mac, M., Real, F. J., Wirz, J., and Von Gunten, U., Photosensitizer method to determine rate constants for the reaction of carbonate radical with organic compounds, *Environ. Sci. Technol.* 39, 9182-9188, 2005.
5. Mack, J., and Bolton, J.R., Photochemistry of nitrite and nitrate in aqueous solution, *J. Photochem. Photobiol. A: Chem.* 128, 1-13, 1999.
6. Sur, B., Rolle, M., Minero, C., Maurino, V., Vione, D., Brigante, M., and Mailhot, G., Formation of hydroxyl radicals by irradiated 1-nitronaphthalene (1NN): oxidation of hydroxyl ions and water by the 1NN triplet state, *Photochem. Photobiol. Sci.*, 10, 1817-1824, 2011.
7. Vermilyea, A.W., and Voelker, B.M., Photo-Fenton reaction at near neutral pH, *Environ. Sci. Technol*., 43, 6927-6933, 2009.
8. Buxton, G.V., Greenstock, C.L., Helman, W.P., and Ross, A.B., Critical review of rate constants for reactions of hydrated electrons, hydrogen atoms and hydroxyl radicals ($^{\bullet}OH/^{\bullet}O^{-}$) in aqueous solution, *J. Phys. Chem. Ref. Data*, 17, 1027-1284, 1988.
9. Brezonik, P.L., and Fulkerson-Brekken, J., Nitrate-induced photolysis in natural waters: Controls on concentrations of hydroxyl radical photo-intermediates by natural scavenging agents, *Environ. Sci. Technol.*, 32, 3004-3010, 1998.
10. Vione, D., Falletti, G., Maurino, V., Minero, C., Pelizzetti, E., Malandrino, M., Ajassa, R., Olariu, R.I., and Arsene, C., Sources and sinks of hydroxyl radicals upon irradiation of natural water samples, *Environ. Sci. Technol.*, 40, 3775-3781, 2006.
11. Bouillon, R.C., and Miller, W.L., Photodegradation of dimethyl sulfide (DMS) in natural waters: Laboratory assessment of the nitrate-photolysis-induced DMS oxidation, *Environ. Sci. Technol.*, 39, 9471-9477, 2005.
12. Canonica, S., Hellrung, B., Muller, P., and Wirz, J., Aqueous oxidation of phenylurea herbicides by triplet aromatic ketones, *Environ. Sci. Technol.*, 40, 6636-6641, 2006.
13. Wenk, J., and Canonica, S., Phenolic antioxidants inhibit the triplet-induced transformation of anilines and sulfonamide antibiotics in aqueous solution, *Environ. Sci. Technol.*, 46, 5455-5462, 2012.
14. Grabner, G., and Richard, C., Mechanisms of direct photolysis of biocides based on halogenated phenols and anilines. In: Boule, P., Bahnemann, D.W., Robertson, P. K. J. (Eds.), *The Handbook of Environmental Chemistry Vol. 2.M – Environmental Photochemistry Part II*, Springer, Berlin, 2005, pp. 161-192.
15. Chiron, S., Minero, C., and Vione, D., Occurrence of 2,4-dichlorophenol and of 2,4-dichloro-6-nitrophenol in the Rhône River Delta (Southern France), *Environ. Sci. Technol.*, 41, 3127-3133, 2007.
16. Chiron, S., Comoretto, L., Rinaldi, E., Maurino, V., Minero, C., and Vione, D., Pesticide by-products in the Rhône delta (Southern France). The case of 4-chloro-2-methylphenol and of its nitroderivative, *Chemosphere*, 74, 599-604, 2009.

17. Maddigapu, P.R., Vione, D., Ravizzoli, B., Minero, C., Maurino, V., Comoretto, L., and Chiron, S., Laboratory and field evidence of the photonitration of 4-chlorophenol to 2-nitro-4-chlorophenol and of the associated bicarbonate effect, *Environ. Sci. Pollut. Res.*, 17, 1063-1069, 2010.
18. Richard, C., and Canonica, S., Aquatic phototransformation of organic contaminants induced by coloured dissolved natural organic matter, In: Boule, P., Bahnemann, D.W., Robertson, P. K. J. (Eds.), *The Handbook of Environmental Chemistry Vol. 2.M – Environmental Photochemistry Part II*, Springer, Berlin, 2005, pp. 299-323.
19. De Laurentiis, E., Chiron, S., Kouras-Hadef, S., Richard, C., Minella, M., Maurino, V., Minero, C., and Vione, D., Photochemical fate of carbamazepine in surface freshwaters: Laboratory measures and modelling, *Environ. Sci. Technol.*, 46, 8164-8173, 2012.
20. Nelieu, S., Perreau, F., Bonnemoy, F., Ollitrault, M., Azam, D., Lagadic, L., Bohatier, J., Einhorn, J., Sunlight nitrate-induced photodegradation of chlorotoluron: Evidence of the process in aquatic mesocosms, *Environ. Sci. Technol.*, 43, 3148-3154, 2009.
21. Machado, F., Collin, L., and Boule, P., Photolysis of bromoxynil (3,5-dibromo-4-hydroxybenzonitrile) in aqueous solution, *Pest. Sci.*, 45, 107-110, 1995.
22. Mansfield, E., and Richard, C., Phototransformation of dichlorophen in aqueous phase, *Pest. Sci.*, 48, 73-76, 1996.
23. Aguer, J.P., Blachère, F., Boule, P., Garaudee, S., and Guillard, C., Photolysis of dicamba (3,6-dichloro-2-methoxybenzoic acid) in aqueous solution and dispersed on solid supports, *Int. J. Photoenergy* 2, 81-86, 2000.
24. Vialaton, D., Baglio, D., Paya-Perez, A., and Richard, C., Photochemical transformation of acifluorfen under laboratory and natural conditions, *Pest. Manag. Sci.*, 57, 372-379, 2001.
25. Torrents, A., Anderson, B.G., Bilboulian, S., Johnson, W.E., and Hapeman, C.J., Atrazine photolysis: Mechanistic investigations of direct and nitrate-mediated hydroxy radical processes and the influence of dissolved organic carbon from the Chesapeake Bay, *Environ. Sci. Technol.*, 31, 1476-1482, 1997.
26. Sakkas, V.A., Lambropoulou, D.A., and Albanis, T.A., Photochemical degradation study of Irgarol 1051 in natural waters: Influence of humic and fulvic substances on the reaction, *J. Photochem. Photobiol. A: Chem.*, 147, 135-141, 2002.
27. Vialaton, D., Pilichowski, J.F., Baglio, D., Paya-Perez, A., Larsen, B., and Richard, C., Phototransformation of propiconazole in aqueous media, *J. Agric. Food Chem.*, 11, 5377-5382, 2001.
28. Hustert, K., Moza, P.N., and Kettrup, A., Photochemical degradation of carboxin and oxycarboxin in the presence of humic substances and soil, *Chemosphere*, 38, 3423-3429, 1999.
29. Krieger, M.S., Yoder, R.N., and Gibson, R., Photolytic degradation of florasulam on soil and in water, *J. Agric. Food Chem.*, 48, 3710-3717, 2000.
30. Bachman, J., and Patterson, H.H., Photodecomposition of the carbamate pesticide carbofuran: Kinetics and the influence of dissolved organic matter, *Environ. Sci. Technol.*, 33, 874-881, 1999.
31. Miller, P.L., and Chin, Y.P., Photoinduced degradation of carbaryl in a wetland surface water, *J. Agric. Food Chem.*, 23, 6758-6765, 2002.
32. Nissenson, P., Dabdub, D., Das, R., Maurino, V., Minero, C., and Vione, D., Evidence of the water-cage effect on the photolysis of NO_3^- and $FeOH^{2+}$. Implications of this effect and of H_2O_2 surface accumulation on photochemistry at the air-water interface of atmospheric droplets, *Atmos. Environ.*, 44, 4859-4866, 2010.
33. Menager, M., and Sarakha, M., Simulated solar light phototransformation of organophosphorus azinphos methyl at the surface of clays and goethite, *Environ. Sci. Technol.*, 47, 765-772, 2013.
34. Faust, B.C., Hoffmann, M.R., and Bahnemann, D.W., Photocatalytic oxidation of sulfur dioxide in aqueous suspensions of α-Fe_2O_3, *J. Phys. Chem.*, 93, 6371-6381, 1989.

35. Serpone, N., and Pelizzetti, E., *Photocatalysis: fundamentals and applications*, Wiley, NY, 1989.
36. Hoffmann, M.R., Martin, S.T., Choi, W.Y., and Bahnemann, D.W., Environmental applications of semiconductor photocatalysis, *Chem. Rev.*, 95, 69-96, 1995.
37. Maurino, V., Minero, C., Mariella, G., and Pelizzetti, E., Sustained production of H_2O_2 on irradiated TiO_2 - fluoride systems, *Chem. Commun.*, 20, 2627-2629, 2005.
38. Vione, D., Maurino, V., Minero, C., Borghesi, D., Lucchiari, M., and Pelizzetti, E., New processes in the environmental chemistry of nitrite. 2. The role of hydrogen peroxide, *Environ. Sci. Technol.*, 37, 4635-4641, 2003.
39. Gieguzynska, E., Amine-Khodja, A., Trubetskoj, O.A., Trubetskaya, O.E., Guyot, G., ter Halle, A., Golebiowska, D., and Richard, C., Compositional differences between soil humic acids extracted by various methods as evidenced by photosensitizing and electrophoretic properties, *Chemosphere*, 75, 1082-1088, 2009.
40. Wang, J.X., Chen, S., Quan, X., and Zhao, Y., Investigation of pentachlorophenol vertical transportation in soil column during its phototransformation on the soil surface, *Wat. Air Soil Pollut.*, 189, 103-112, 2008.
41. Ter Halle, A., Drncova, D., and Richard, C., Phototransformation of the herbicide sulcotrione on maize cuticular wax, *Environ. Sci. Technol.*, 40, 2989-2995, 2006.
42. Lavieille, D., ter Halle, A., and Richard, C., Understanding mesotrione photochemistry when applied on leaves, *Environ. Chem.*, 5, 420-425, 2008.
43. Eyheraguibel, B., Ter Halle, A., and Richard, C., Photodegradation of bentazon, clopyralid, and triclopyr on model leaves: Importance of a systematic evaluation of pesticide photostability on crops, *J. Agric. Food Chem.*, 57, 1960-1966, 2009.
44. Ter Halle, A., Lavieille, D., and Richard, C., The effect of mixing two herbicides mesotrione and nicosulfuron on their photochemical reactivity on cuticular wax film, *Chemosphere*, 79, 482-487, 2010.
45. Monadjemi, S., El Roz, M., Richard, C., and Ter Halle, A., Photoreduction of chlorothalonil fungicide on plant leaf models, *Environ. Sci. Technol.*, 45, 9582-9589, 2011.
46. Monadjemi, S, Ter Halle, A., and Richard, C., Reactivity of cycloxydim toward singlet oxygen in solution and on wax film, *Chemosphere*, 89, 269-273, 2012.
47. Vione, D., Maurino, V., Minero, C., Pelizzetti, E., Harrison, M.A.J., Olariu, R.I., and Arsene, C., Photochemical reactions in the tropospheric aqueous phase and on particulate matter, *Chem. Soc. Rev.*, 35, 441–453, 2006.
48. Hoffmann, M.R., Homogeneous and heterogeneous photochemistry in the atmosphere, In: Boule, P., Bahnemann, D.W., Robertson, P. K. J. (Eds.), *The Handbook of Environmental Chemistry Vol. 2.M – Environmental Photochemistry Part II*, Springer, Berlin, 2005, pp. 77-118.
49. Wallington, T.J., and Nielsen, O.J., Atrmospheric photooxidation of gas phase air pollutants, In: Boule, P., Bahnemann, D.W., Robertson, P. K. J. (Eds.), *The Handbook of Environmental Chemistry Vol. 2.M – Environmental Photochemistry Part II*, Springer, Berlin, 2005, pp. 119-160.
50. Borghesi, D., Vione, D., Maurino, V., and Minero, C., Transformations of benzene photoinduced by nitrate salts and iron oxide, *J. Atmos. Chem.*, 52, 259-281, 2005.
51. Maurino, V., Bedini, A., Borghesi, D., Vione, D., and Minero, C., Phenol transformation photosensitised by quinoid compounds, *Phys. Chem. Chem. Phys.*, 13, 11213-11221, 2011.
52. Brigante, M., Charbouillot, T., Vione, D., and Mailhot, G., Photochemistry of 1-nitronaphthalene: A potential source of singlet oxygen and radical species in atmospheric waters, *J. Phys. Chem. A*, 114, 2830–2836, 2010.
53. Albinet, A., Minero, C., and Vione, D., Photochemical generation of reactive species upon irradiation of rainwater: Negligible photoactivity of dissolved organic matter, *Sci. Total Environ.*, 408, 3367-3373, 2010.

54. Parazols, M., Marinoni, A., Amato, P., Abida, O., Laj, P., and Mailhot, G., Speciation and role of iron in cloud droplets at the puy de Dome station, *J. Atmos. Chem.*, 54, 267-281, 2006.
55. Marinoni, A., Parazols, M., Brigante, M., Deguillaume, L., Amato, P., Delort, A.M., Laj, P., and Mailhot, G., Hydrogen peroxide in natural cloud water: Sources and photoreactivity, *Atmos. Res.*, 101, 256-263, 2011.
56. Vione, D., Maurino, V., Minero, C., Pelizzetti, E., The atmospheric chemistry of hydrogen peroxide: A review, *Ann. Chim. (Rome)*, 93, 477-488, 2003.
57. Warneck, P., The relative importance of various pathways for the oxidation of sulphur dioxide and nitrogen dioxide in sunlit continental fair weather clouds, *Phys. Chem. Chem. Phys.*, 1, 5471-5483, 1999.
58. Vione, D., Das, R., Rubertelli, F., Maurino, V., Minero, C., Barbati, S., and Chiron, S., Modelling the occurrence and reactivity of hydroxyl radicals in surface waters: Implications for the fate of selected pesticides, *Intern. J. Environ. Anal. Chem.*, 90, 258-273, 2010.
59. Frank, R., and Klöpffer, W., Spectral solar photo irradiance in Central Europe and the adjacent north Sea, *Chemosphere*, 17, 985-994, 1988.
60. Vione, D., Khanra, S., Cucu Man, S., Maddigapu, P.R., Das, R., Arsene, C., Olariu, R.I., Maurino, V., and Minero, C., Inhibition vs. enhancement of the nitrate-induced phototransformation of organic substrates by the $^{\bullet}OH$ scavengers bicarbonate and carbonate, *Wat. Res.* 43, 4718-4728, 2009.
61. Minero, C., Chiron, S., Falletti, G., Maurino, V., Pelizzetti, E., Ajassa, R., Carlotti, M.E., and Vione, D., Photochemical processes involving nitrite in surface water samples, *Aquat. Sci.* 69, 71-85, 2007.
62. Vione, D., Feitosa-Felizzola, J., Minero, C., and Chiron, S., Phototransformation of selected human-used macrolides in surface water: Kinetics, model predictions and degradation pathways. *Wat. Res.* 43, 1959-1967, 2009.
63. Vione, D., Minella, M., Minero, C., Maurino, V., Picco, P., Marchetto, A., and Tartari, G., Photodegradation of nitrite in lake waters: role of dissolved organic matter, *Environ. Chem.*, 6, 407-415, 2009.
64. Vione, D., Maurino, V., Minero, C., Carlotti, M.E., Chiron, S., and Barbati, S., Modelling the occurrence and reactivity of the carbonate radical in surface freshwater, *C. R. Chimie*, 12, 865-871, 2009.
65. Vione, D., Das, R., Rubertelli, F., Maurino, V., and Minero, C., Modeling of indirect phototransformation processes in surface waters. In: *Ideas in Chemistry and Molecular Sciences: Advances in Synthetic Chemistry*, Pignataro, B., ed., Wiley-VCH, Weinheim, Germany, 2010, pp. 203-234.
66. Al-Housari, F., Vione, D., Chiron, S., and Barbati, S., Reactive photoinduced species in estuarine waters. Characterization of hydroxyl radical, singlet oxygen and dissolved organic matter triplet state in natural oxidation processes, *Photochem. Photobiol. Sci,* 9, 78-86, 2010.
67. Zertal, A., Sehili, T., and Boule, P., Photochemical behaviour of 4-chloro-2-methylphenoxyacetic acid: Influence of pH and irradiation wavelength*, J. Photochem. Photobiol. A: Chem.*, 146, 37-48, 2001.
68. Vione, D., Khanra, S., Das, R., Minero, C., Maurino, V., Brigante, M., and Mailhot, G., Effect of dissolved organic compounds on the photodegradation of the herbicide MCPA in aqueous solution, *Wat. Res.*, 44, 6053-6062, 2010.
69. Benitez, F.J., Acero, J.L., Real, F.J., Roman, S., Oxidation of MCPA and 2,4-D by UV radiation, ozone, and the combinations UV/H_2O_2 and O_3/H_2O_2, *J. Environ. Sci. Health B*, 39, 393-409, 2004.